Structural analysis of a scissor structure

I. ARIO [1*] , T. YAMASHITA[1], Y. CHIKAHIRO[2], M. NAKAZAWA[3], K. FEDOR[4],
C. GRACZYKOWSKI[4*], and P. PAWŁOWSKI[4*]

[1] Hiroshima University, 1-4-1 Kagamiyama Higashi-hiroshima, Japan
[2] Shinshu University, Nagano, Japan
[3] Tohoku Gakuin University, Tagajo, Japan
[4] Institute of Fundamental Technological Research, Polish Academy of Sciences, ul. Pawińskiego 5B, 02-106 Warsaw, Poland

Abstract. This paper presents equilibrium mechanics and a finite element model for analysing a scissor structure that contains pivots with zero bending stiffness representing structural instability. The pivot at the centre of each structural unit, which is a feature of scissor structures, can be used to transfer the displacement between the units. It cannot, however, transfer the rotation between these units, and the angular stiffness must be considered independently for each unit. To construct a general model of the scissor structure, a scissor unit was developed using the left and right boundary connections of adjacent units to simulate a periodically symmetric structure. The proposed method allows us to obtain an accurate distribution of the internal forces and deflections without the use of special elements to account for central pivots.

Key words: scissor structure, deployable structure, smart bridge, scissors finite element, equilibrium mechanics.

1. Introduction

The chain scissor structure mechanism, a well-known principle for expanding and contracting a structure, is widely used for space structures, machines (lifters), and building structures (tents, gates, etc.). There is a great engineering utility value in a structure that can expand by itself. A mathematical model that governs its mechanics is required to design a general-purpose structure. In general, to analyse the scissor structure, it is necessary to impose the boundary conditions. To solve the zero-stiffness problem with the pin connection of the scissor structure, we propose the solution of the equilibrium equation derived from the equilibrium condition of a free-body diagram (FBD) with the nodal forces at the scissor connection points. For more complex, statically indeterminate scissor structure, we have developed a new analysis method based on the finite element method (FEM).

We consider a structural analysis to introduce this chain scissor into a prefabricated bridge easily, quickly, and safely with infrastructural structures. This eliminates the need for on-site bridge assembly, and the process is quick and efficient. To achieve this approach, a lightweight, high-strength bridge system is also generally required [1–5]. Therefore, a method must be developed to determine the optimal layout, shape, and design of these bridges to ensure that the structural form of the bridge system exhibits high stiffness [6,7]. To date, many structural optimisation theories have been developed in an attempt to ensure both a lightweight [8] and highly rigid design. Moreover, the

application of adaptive elements with controllable mechanical characteristics enables obtaining adaptability and deformation control under actual static or dynamic loading [9].

In this paper, we proposed a new, pre-assembled smart bridge [10–15]. Previous studies have proposed methods to determine the cross-sectional forces for all elements based on *equilibrium mechanics* for a unit of a linked scissor structure. The displacements of the nodal points of the scissor structure have also been determined by structural analyses, such as by the unit load method and/or minimum strain energy methods. This bridge has a scissor structure that enables quick deployment via a collapsible structural frame. It was structurally optimised using a reinforced scissor system. Except the authors's theory of *equilibrium mechanics*, no method for analysing such a bridge has been proposed; the scissor system in this bridge contains pin-joint structures that possess zero-stiffness and represent a structural instability.

Scissor-type periodic structures are extremely useful in building a quickly deployable bridge. The scissor bridge constructed of several scissor units can be considered as a periodic structure. Periodic structures, such as honeycomb structures, are also called *cell structures*, and their basic units are called *unit cells*. As computational power has increased, structural analysis can be performed using the FEM [16, 17]. Therefore, the use of FEM (which incorporates multi-scale analysis, the homogenisation method, extended truss theory including scissor structures [18], etc.) with a unit cell as a representative volume element (RVE) was proposed by C.T. Sun [19] *et al.* to analyse such structures. Following such an approach, in this analysis, we focused on the topology of the microtruss structure using the microtruss analytical method [10], considering the symmetry present in periodic structures. The discretised periodic structure [20, 21] was analysed via the FEM and treated

I. Ario, T. Yamashita, Y. Chikahiro, M. Nakazawa, K. Fedor, C. Graczykowski, and P. Pawłowski

as a cell structure, and the issue of building a fundamental scissor element using the FEM was also considered.

In this study, discrete FEM elements with many degrees of freedom, which prevent structural instability and allow to change support and load conditions freely, were developed taking into account the periodicity of the analysed structure. Using the periodic units of the scissor structure as representative units, the stiffness of the entire structure was analysed via the RVE method [22]. After discretising n units of the scissor structure to represent the overall scissor structure, a FEM element consisting of these scissor units was constructed. Thus, a complete FEM model with n scissor units could be developed. A new, cell-based FEM that avoids indefinite numerical solutions for scissor structures was developed, and accurate deformation information was obtained using the proposed method without the need for special elements to represent pivots.

The accuracy of the proposed method was verified by analysing displacements and the cross-sectional forces for each member and comparing it with the results obtained by using the present theories and ABAQUS software computation for a scissors structures. The significant result of this study is development of the analysis method for scissors structures and/or frame elements with different pin connections for the periodic modular elements using the FEM. Finally, the merits of three present methods including equilibrium mechanics model, developed models of scissors structures and ABAQUS FEM models have been summarized in the concluding section.

2. Equilibrium mechanics for the scissor structure

In this section, we introduce a part of the theoretical solution approach called *equilibrium mechanics* for a single scissor structure unit [23].

2.1. Equilibrium equibalance of a scissor unit. First, a free-body diagram (FBD) of a scissor structure is shown in Fig. 1.
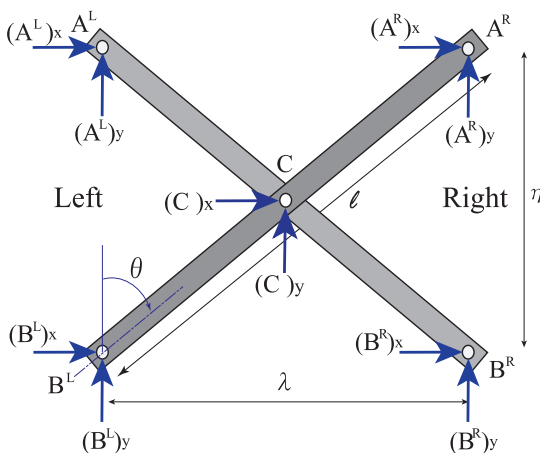
Fig. 1. The definition of equilibrium mechanics for a unit of scissor structure

It is assumed that the length of each member is ℓ and the inclination angle is θ measured clockwise from the vertical direction; the span λ and the height η are related by $\lambda = \ell \sin \theta$ and $\eta = \ell \cos \theta$.

Thus, the configuration of such a structure can be represented by the angle θ. This scissor structure with five nodal points with nodes named as A^L, B^L, C, A^R, B^R, can be analysed by using the equilibrium equations for the FBD of Fig. 1. The equilibrium equation for each external force[1] in the x and y direction is as follows:

$$\Sigma H : \quad (A^L)_x + (B^L)_x + (C)_x + (A^R)_x + (B^R)_x = 0, \quad (1)$$

$$\Sigma V : \quad (A^L)_y + (B^L)_y + (C)_y + (A^R)_y + (B^R)_y = 0. \quad (2)$$

For the intersecting members, $\overline{B^L A^R}$ and $\overline{B^R A^L}$, two equilibrium equations can be obtained for the moments at point C:

$$\Sigma M_C : \quad -\frac{\eta}{2}(B^L)_x + \frac{\lambda}{2}(B^L)_y + \frac{\eta}{2}(A^R)_x - \frac{\lambda}{2}(A^R)_y = 0, \quad (3)$$

$$\Sigma M_C : \quad -\frac{\eta}{2}(B^R)_x - \frac{\lambda}{2}(B^R)_y + \frac{\eta}{2}(A^L)_x + \frac{\lambda}{2}(A^L)_y = 0. \quad (4)$$

Let us consider the case of a simple cantilever model that has pinned supports at points A^L and B^L. The equilibrium of such a structure can be written in the form of a matrix equation based on the equilibrium equations derived above (Eq. (1) to Eq. (4)).

$$L \begin{bmatrix} (B^L)_x \\ (B^L)_y \\ \hline (A^L)_x \\ (A^L)_y \end{bmatrix} = -R \begin{bmatrix} (B^R)_x \\ (B^R)_y \\ \hline (A^R)_x \\ (A^R)_y \end{bmatrix} - \begin{bmatrix} (C)_x \\ (C)_y \\ 0 \\ 0 \end{bmatrix}$$

$$\begin{bmatrix} (B^L)_x \\ (B^L)_y \\ \hline (A^L)_x \\ (A^L)_y \end{bmatrix} = -L^{-1}R \begin{bmatrix} (B^R)_x \\ (B^R)_y \\ \hline (A^R)_x \\ (A^R)_y \end{bmatrix} - S \begin{bmatrix} (C)_x \\ (C)_y \end{bmatrix}, \quad (5)$$

where

$$L = \begin{bmatrix} 1 & 0 & 1 & 0 \\ 0 & 1 & 0 & 1 \\ \hline -\eta & \lambda & 0 & 0 \\ 0 & 0 & \eta & \lambda \end{bmatrix}, \qquad R = \begin{bmatrix} 1 & 0 & 1 & 0 \\ 0 & 1 & 0 & 1 \\ \hline 0 & 0 & \eta & -\lambda \\ -\eta & -\lambda & 0 & 0 \end{bmatrix},$$

---

[1] This means that a force at the nodal point is $(\bullet^*)_\Phi$, $(\bullet^*)_\Phi \equiv [\bullet^* | A^L, B^L, C, A^R, B^R; * = \{L, R\}; \Phi = \{x, y\}]$, $\bullet^*$ is nodal label.

$$L^{-1}R = \begin{bmatrix} 1 & \dfrac{\lambda}{\eta} & 0 & \dfrac{\lambda}{\eta} \\ \dfrac{\eta}{\lambda} & 1 & \dfrac{\eta}{\lambda} & 0 \\ \hline 0 & -\dfrac{\lambda}{\eta} & 1 & -\dfrac{\lambda}{\eta} \\ -\dfrac{\eta}{\lambda} & 0 & -\dfrac{\eta}{\lambda} & 1 \end{bmatrix},$$

$$S = \begin{bmatrix} \dfrac{1}{2} & \dfrac{\lambda}{2\eta} \\ \dfrac{\eta}{2\lambda} & \dfrac{1}{2} \\ \hline \dfrac{1}{2} & -\dfrac{\lambda}{2\eta} \\ -\dfrac{\eta}{2\lambda} & \dfrac{1}{2} \end{bmatrix}.$$

These equilibrium equations obtain the left nodal forces (B^L) and (A^L) at points B^L and A^L for the right and central nodal forces (B^R), (A^R), and (C), which are given as the load values. Therefore, the axial force, shear force, and bending moment can be calculated based on the projection of the above nodal forces to the member directions.

2.2. Structural analysis for nodal displacements. We consider a simple model of the scissor-type bridge by using the equilibrium equation method to introduce the mechanical properties, definition of nodes, and internal forces N_j, Q_j, M_j, which are calculated by the projection of the above nodal forces on the member direction (FBD shown in Fig. 2(a)). We assume that

(a) FBD of a unit of scissor

(b) A two-unit scissor structure under the loadings Q, P
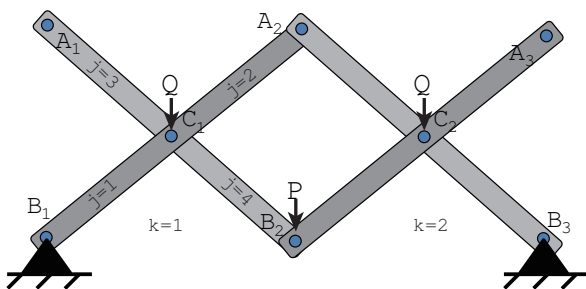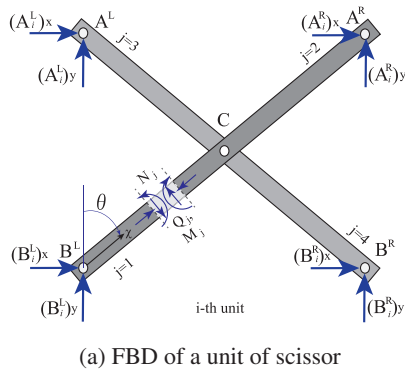
Fig. 2. Models of scissors structures

there are two units of the scissor structure with a simple support as shown in Fig. 2(b) and their internal forces N_j, Q_j, M_j are obtained based on the equilibrium equation method. The length of all members is $\ell = \sqrt{\eta^2 + \lambda^2}$ in which, η is the vertical height and λ is the horizontal distance for a unit. We consider that the vertical nodal displacement $v_\bullet$ depends on the loading at nodal points of n-units of the scissor structure according to the unit load method in the following way:

$$v_\bullet = \sum_{k=1}^{n} \sum_{j=1}^{4} \int_0^{\ell_j^k/2} \left(\frac{N_{0j}^k \overline{N_{\bullet j}^k}}{EA} + \kappa \frac{Q_{0j}^k \overline{Q_{\bullet j}^k}}{GA} \right.$$
$$\left. + \frac{M_{0j}^k(\chi)\overline{M_{\bullet j}^k(\chi)}}{EI} \right) \mathrm{d}\chi, \qquad (6)$$

where χ is the distance from each corner nodal point in Fig. 3(a). N_0, $\overline{N_\bullet}$ are the internal axial force in the member caused by the real loads and the internal virtual force caused by the external virtual unit load, respectively; Q_0, $\overline{Q_\bullet}$ are the internal shear force in the member and internal virtual shear, respectively; κ is the form factor for the cross-sectional area; M_0, $\overline{M_\bullet}$ are internal moments in the frame and the internal virtual moment, respectively; k is the number of units; and j is the number of half units of the member. We can consider several scissor structure units with the coupling conditions of a linked scissor structure. For example, in the case of two units $(n = 2)$ in the FEM shown in Fig. 2(b), the virtual moment $\overline{M_{\bullet j}^k}$ under $\overline{P}_\bullet = 1$ at each nodal point is used to obtain a nodal displacement of $v_\bullet$. As the shear effect is small and the corresponding term can be neglected, Eq. (6) is expressed as

$$v_\bullet = \sum_{k=1}^{2} \sum_{j=1}^{4} \left(\frac{N_{0j}^k \overline{N_{\bullet j}^k}}{EA} \frac{\ell_j^k}{2} + \int_0^{\ell_j^k/2} \frac{M_{0j}^k(\chi)\overline{M_{\bullet j}^k(\chi)}}{EI} \mathrm{d}\chi \right),$$
$$\text{at points } \bullet = \{C_1, B_2, C_2, A_2, A_1, A_3\}. \qquad (7)$$

the virtual moment $\overline{M_{\bullet j}^k} = 1$ at each nodal point to obtain nodal the deformed angle $\phi_\bullet$ in the following:

$$\phi_\bullet = \sum_k \sum_{j=1}^{4} \int_0^{\ell_j^k/2} \frac{M_{0j}^k(\chi)\overline{M_{\bullet j}^k}}{EI} \mathrm{d}\chi, \quad \text{at points } \bullet = \{C_1, C_2\}. \qquad (8)$$

Thus, the mechanical method based on the equilibrium mechanics of a scissor unit allows us to obtain the displacement, including the rotation, of every node of the scissor structure.

3. FEM analysis of the scissor units

Second, we suggest the FEM, which allows us to assemble the equilibrium equation with the stiffness matrix for units of scissor structure. In this paper, the following assumptions are made regarding the construction method of a scissors element and the analytical conditions for the application of the FEM.

I. Ario, T. Yamashita, Y. Chikahiro, M. Nakazawa, K. Fedor, C. Graczykowski, and P. Pawłowski

- The scissors element is constructed using a static approach proposed in the analysis of periodic structures. This methodology and analysis method is used only for the functional simplification of joints. However, the accuracy of the method is affected by stiffness of such connections.
- In fact, the actual scissor structures include various types of non-linear phenomena in the joints (contact, clearance, friction). Nonlinear functions, such as the effect of friction and contact issues, are not considered in this analytical model. A precise mapping of the articulated joints enables the advanced static and dynamic analysis of this type of structure. This complex situation requires the extensive use of FEM, but is not within the scope of this paper.

In general, the discretised equilibrium equation of a standard FEM containing N degrees-of-freedom of all frame elements in global coordinate system (GCS) is described by

$$F(f,u) \equiv Ku - f = 0, \qquad (9)$$

where F is the defined equilibrium equation, $K \in \mathbf{R}^{N \times N}$ is the stiffness matrix, $u \in \mathbf{R}^N$ is the vector of nodal displacements and $f \in \mathbf{R}^N$ is the vector of nodal loads.

The stiffness equation in the Element Coordinate System (ECS) is the following:

$$f^e = \overline{k}^e u^e,$$

$$\begin{bmatrix} f_i^e \\ f_j^e \end{bmatrix} = \begin{bmatrix} \overline{k}_{ii}^e & \overline{k}_{ij}^e \\ \overline{k}_{ji}^e & \overline{k}_{jj}^e \end{bmatrix} \begin{bmatrix} u_i^e \\ u_j^e \end{bmatrix} \quad \text{in ECS,} \qquad (10)$$

here $f^e \in \mathbf{R}^6$ is a vector of the internal nodal forces for the local frame element. $\overline{k}_{ij}^e$ is the component i, j of the stiffness matrix $\overline{k}^e \in \mathbf{R}^{6 \times 6}$ for an element, EI is the bending stiffness, EA is the axial stiffness for structural members in ECS $\overline{k}^e$ is defined as follows:

$$\overline{k}^e = \begin{bmatrix} \dfrac{EA}{\ell} & & & & & \\ 0 & \dfrac{12EI}{\ell^3} & & \text{Symm.} & & \\ 0 & \dfrac{6EI}{\ell^2} & \dfrac{4EI}{\ell} & & & \\ -\dfrac{EA}{\ell} & 0 & 0 & \dfrac{EA}{\ell} & & \\ 0 & -\dfrac{12EI}{\ell^3} & -\dfrac{6EI}{\ell^2} & 0 & \dfrac{12EI}{\ell^3} & \\ 0 & \dfrac{6EI}{\ell^2} & \dfrac{2EI}{\ell} & 0 & -\dfrac{6EI}{\ell^2} & \dfrac{4EI}{\ell} \end{bmatrix}. \qquad (11)$$

In this method, we focus on a set of units in the entire linked scissor structure with the same length ℓ. It is assumed that in all members, each unit of the scissor structure is constructed in the same manner. The deformation of this structure can be analysed by determining the stiffness matrix K that expresses the relationship between the displacement and load at the state of equilibrium. A scissor structure is composed of scissor units that consist of a pair of straight bars affected by both the axial

forces and the bending moments. An 'X'-shaped scissor unit is composed of four elements, m, which are described in terms of the nodes denoted by i and j for each frame element.

3.1. Transformation through the scissor coordinate system (SCI). One scissor unit system is comprised of 4 individual elements shown in Fig. 3(a), and these 4 elements should be combined to represent a coordinate system (SCI) per a scissor element in this paper[2]. As shown in Fig. 3(b), the FEM of the scissors unit comprises a configuration of four degrees of freedom of the extended nodal force vector and the displacement vector at each nodal point of the unit scissors structure. If the scissors structure has no pin joints and is a rigidly connected frame element, the two rotational degrees of freedom have a common rotational displacement and each node then has three degrees of freedom. A coordinate transformation matrix, $T(\varphi_m)$, is defined using inclination angles φ_m of the elements in the initial configuration. The stiffness matrix $k^{(m)}$ is transformed from the element coordinate system to scissor element system using the coordinate transformation matrix, $T(\varphi_m)$. The transformation is obtained using the following equation:

$$k^{(m)} = \mathscr{T}_m^{\mathrm{T}} \overline{k}^e \mathscr{T}_m$$
$$= \begin{bmatrix} k_{ii}^{(m)} & k_{ij}^{(m)} \\ k_{ji}^{(m)} & k_{jj}^{(m)} \end{bmatrix} \quad \text{from ECS to SCI,} \qquad (12)$$

where $k^{(m)}$ is the stiffness matrix after local transposition. The ends of each element $(m = 1, \cdots, 4)$ correspond to the nodal points i and j shown in Fig. 3 in the following way:

$$k^{(1)} = \begin{bmatrix} k_{11}^{(1)} & k_{13}^{(1)} \\ k_{31}^{(1)} & k_{33}^{(1)} \end{bmatrix}, \quad \cdots, \quad k^{(4)} = \begin{bmatrix} k_{33}^{(4)} & k_{35}^{(4)} \\ k_{53}^{(4)} & k_{55}^{(4)} \end{bmatrix}.$$

Then, the transformation matrix $\mathscr{T}_m$ is defined as follows:

$$\mathscr{T}_m = \begin{bmatrix} T(\varphi_m) & O \\ O & T(\varphi_m) \end{bmatrix}, \text{ where} \qquad (13)$$

$$T(\varphi_m) = \begin{bmatrix} \cos(\varphi_m) & \sin(\varphi_m) & 0 & 0 \\ -\sin(\varphi_m) & \cos(\varphi_m) & 0 & 0 \\ 0 & 0 & a & b \end{bmatrix},$$

$$\text{here} \quad \begin{array}{cc|c} a & b & \text{element no.} \\ \hline 1 & 0 & \text{for } m = 1,4 \\ 0 & 1 & \text{for } m = 2,3 \end{array}. \qquad (14)$$

The stiffness matrix and transformation matrix from ECS to SCI is expanding the size of stiffness matrix $K^{(1)}$ for a unit of a scissor element, with the size of the elemental stiffness matrix $k^{(m)}$ as a part of a scissor unit from 16 to 20 degrees-of-freedom of a frame element. It is defined by expanding stiffness matrices as $K_{sc}^{(M)}$ for the M-th unit of a scissor FEM element with four

---

[2]This coordinate system (SCI) can be used to represent rigid frames with different connections based on the periodic cell structure.

(a) A scissor element system (SCI)

(b) Degrees of freedom in a unit
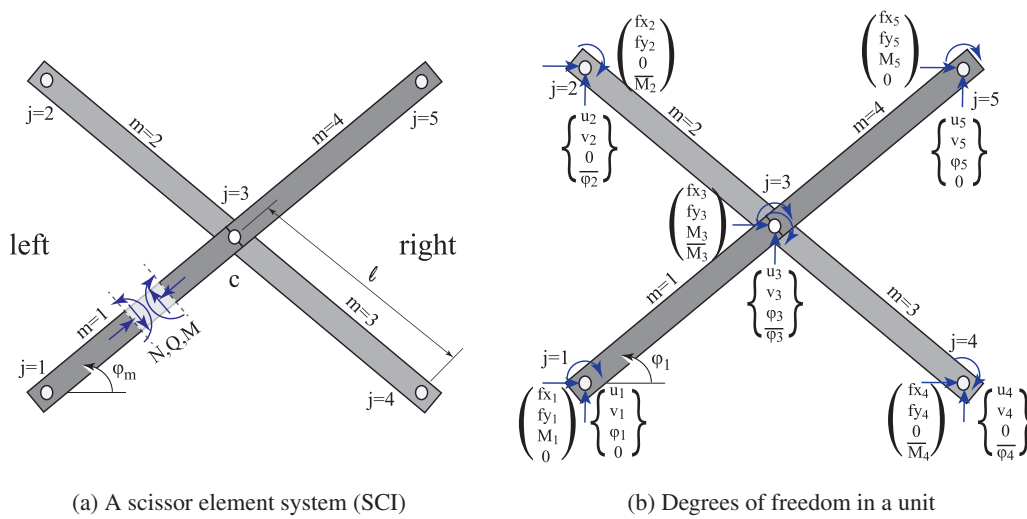
Fig. 3. FEM for a scissors unit combined by 4 frame elements ($m = 1, \cdots, 4$)

frame elements after transforming local stiffness matrix $k^{(m)}$ in the following way:

$$K_{sc}^{(M)} \equiv \sum_{m=1}^{4} \left[k^{(m)} \right] \quad \text{from SCI to GCS}$$

$$= \sum_{m=1}^{4} \begin{bmatrix} \cdot & \cdot & \cdot & \cdot & \cdot \\ \cdot & k_{ii}^{(m)} & \cdot & k_{ij}^{(m)} & \cdot \\ \cdot & \cdot & \cdot & \cdot & \cdot \\ \cdot & k_{ji}^{(m)} & \cdot & k_{jj}^{(m)} & \cdot \\ \cdot & \cdot & \cdot & \cdot & \cdot \end{bmatrix},$$

$$\{(i,j) \text{ or } (j,i) | (1,3), (2,3), (4,3), (5,3)\}$$
$$\cup \{(i,i) \text{ or } (j,j), i \neq j | i, j = 1, \cdots, 5\}$$

$$= \begin{bmatrix} k_{11}^{(1)} & O & k_{13}^{(1)} & O & O \\ O & k_{22}^{(2)} & k_{23}^{(2)} & O & O \\ k_{31}^{(1)} & k_{32}^{(2)} & \sum_{m=1}^{4} k_{33}^{(m)} & k_{34}^{(3)} & k_{35}^{(4)} \\ O & O & k_{43}^{(3)} & k_{44}^{(3)} & O \\ O & O & k_{53}^{(4)} & O & k_{55}^{(4)} \end{bmatrix}, \quad (15)$$

where the stiffness matrix of a unit of scissor might be determined by using (15). Any diagonal components $k_{jj}^{(m)}$, $j = 1, \cdots, 5$ of the stiffness matrix $K_{sc}^{(M)}$ in a scissor unit are not zero, and they should assume positive values. The pivot at the centre of the scissor unit is used to determine the displacement between the 4 elements, but not the rotation. The stiffness resulting from the whole structural system consisting of each element can be placed in the matrix location corresponding to that element; however, the stiffness resulting from the rotation of each element must be inputted using additional columns and rows. Specifically, when the stiffness corresponding to the pin

joint is included, a matrix $k_{ij}^{(m)} \in \mathbf{R}^{4 \times 4}$ is required. Following the RVE method, we consider the set of unit elements of the same geometry and scale, which are described by the stiffness matrices:

$$K_{sc}^{(1)} = \cdots = K_{sc}^{(M)} = \cdots = K_{sc}^{(n)}. \quad (16)$$

The stiffness corresponding to the rightmost connection of the scissor unit is shown in the lower right corner of the matrix, and the stiffness corresponding to the leftmost connection is shown in the upper left corner.

4. Determining the stiffness of n scissor units

The stiffness of n scissor units can be obtained by examining the stiffness of one scissor unit with respect to the left and right connected conditions and assembling the global stiffness matrix of the system as follows:

$$K_{sc} = \sum_{M=1}^{n} \left[K_{sc}^{(M)} \right] \quad \text{in GCS}$$

$$= \sum_{M=1}^{n} \begin{bmatrix} \cdot & \cdot & \cdot & \cdot & \cdot \\ \cdot & \left[K_{sc}^{(M)} \right]_{ll} & \cdot & \left[K_{sc}^{(M)} \right]_{lr} & \cdot \\ \cdot & \cdot & \cdot & \cdot & \cdot \\ \cdot & \left[K_{sc}^{(M)} \right]_{rl} & \cdot & \left[K_{sc}^{(M)} \right]_{rr} & \cdot \\ \cdot & \cdot & \cdot & \cdot & \cdot \end{bmatrix}$$

$$= \begin{bmatrix} \left[K_{sc}^{(1)} \right]_{ll} & \left[K_{sc}^{(1)} \right]_{lr} & & \\ \left[K_{sc}^{(1)} \right]_{rl} & \left[K_{sc}^{(1)} \right]_{rr} + \left[K_{sc}^{(2)} \right]_{ll} & \ddots & \\ & & (M) & \ddots \\ & & \ddots & \left[K_{sc}^{(n)} \right]_{rr} \end{bmatrix}, \quad (17)$$

I. Ario, T. Yamashita, Y. Chikahiro, M. Nakazawa, K. Fedor, C. Graczykowski, and P. Pawłowski

$$
= \begin{bmatrix} K_{sc}^{(1)} & K_{sc}^{(1)} & & & & & \\ K_{sc}^{(1)} & K_{sc}^{(1)}+K_{sc}^{(2)} & K_{sc}^{(2)} & & & & \\ & K_{sc}^{(2)} & K_{sc}^{(2)}+K_{sc}^{(3)} & K_{sc}^{(3)} & & & \\ & & K_{sc}^{(3)} & K_{sc}^{(3)}+ & \ddots & & \\ & & & & {}^{(M)} & & \\ & & & \ddots & \ddots & \ddots & \\ & & & & \ddots & +K_{sc}^{(n)} & K_{sc}^{(n)} \\ & & & & & K_{sc}^{(n)} & K_{sc}^{(n)} \end{bmatrix}
$$

$$
= \begin{bmatrix} \cdot & \cdot & \cdot & \cdot & \cdot \\ \cdot & [K_{sc}]_{ii} & \cdot & [K_{sc}]_{ij} & \cdot \\ \cdot & \cdot & \cdot & \cdot & \cdot \\ \cdot & [K_{sc}]_{ji} & \cdot & [K_{sc}]_{jj} & \cdot \\ \cdot & \cdot & \cdot & \cdot & \cdot \end{bmatrix}, \tag{18}
$$

where in equation (17), l and r for $\circ$ and/or $\bullet$ of $[K_{sc}^{(M)}]_{\circ\bullet}$ superscripts $\circ\bullet$, denote the components that correspond to the left connection and right connection, respectively. The stiffness of one scissor unit is used to determine the global stiffness of n scissor units that overlap periodically. Because the leftmost and rightmost connections of a scissor unit are connected by pin joints to the bordering units, the longitudinal and transverse stiffnesses of each unit at these boundaries are the same and are in the same cell of the matrix. However, the stiffnesses associated with the rotation are specific to each unit, and thus are placed in separate locations in the stiffness matrix. In this study, three connecting scissor units are used to represent n scissor units.

5. Reinforcement of the scissor structure

In this section, we consider a structural model with a reinforced member which is not a frame member after the stable expanding scissors bridge, which is supported at its ends. As the applied reinforcement resists only the axial force and not the bending moment, the stiffness related to the axial force alone is changed in the stiffness matrix. The overall stiffness matrix is combined with the chained frame stiffness matrix K_{sc} of equation (17) and the sectional stiffness from $\bar{k}_{EB}^{e}$ without any bending stiffness EI of the reinforcement element. While considering the local stiffness of the reinforced member, the total stiffness matrix K_{sc}^{*} is defined as follows:

$$
K_{sc}^{*} = K_{sc} + \sum_{m} K_{EB}^{(m)} \quad \text{in GCS}
$$

$$
= K_{sc} + \sum_{m} \begin{bmatrix} \cdot & \cdot & \cdot & \cdot & \cdot \\ \cdot & \left[k_{EB}^{(m)}\right]_{ii} & \cdot & \left[k_{EB}^{(m)}\right]_{ij} & \cdot \\ \cdot & \cdot & \cdot & \cdot & \cdot \\ \cdot & \left[k_{EB}^{(m)}\right]_{ji} & \cdot & \left[k_{EB}^{(m)}\right]_{jj} & \cdot \\ \cdot & \cdot & \cdot & \cdot & \cdot \end{bmatrix}, \tag{19}
$$

here $k^{e}|_{EI=0}$ is substituting $EI = 0$ for Eq. (12) in the following:

$$
K_{EB}^{(m)} = \left[k_{EB}^{(m)}\right] \quad \text{from SCI to GCS}
$$

$$
k_{EB}^{(m)} = \mathscr{T}_{m}^{\mathrm{T}} \bar{k}^{e}\Big|_{EI=0} \mathscr{T}_{m} = \begin{bmatrix} \left[k_{EB}^{(m)}\right]_{ii} & \left[k_{EB}^{(m)}\right]_{ij} \\ \left[k_{EB}^{(m)}\right]_{ji} & \left[k_{EB}^{(m)}\right]_{jj} \end{bmatrix}
$$

from ECS to SCI.

6. Superelement model of scissor unit

The approach alternative to application of the classical stiffness matrix of a single scissors unit is construction of a "superelement" that models a single scissors unit. The main difference between both approaches is the number of nodes and the number of corresponding degrees of freedom used for scissors unit modelling. In a classical FEM approach a single scissors unit has five standard nodes (four nodes at the ends of scissors members and one node at central pivot). In turn, the scissors unit "superelement" has four external nodes ($j = 1, 2, 4, 5$ in Fig. 3) located at the ends of the scissors members and one internal node ($j = 3$ in Fig. 3) at the central pivot. The external nodes collect external degrees of freedom, while the internal nodes collect internal degrees of freedom.

The methodology of constructing scissors units "superelement" is analogous to development of other "superelements" known in FEM. The scissors unit "superelement" is obtained directly from the FEM model of a single scissors unit through elimination of the internal dofs and expressing them in terms of external dofs. Mathematically, the procedure of derivation of the superelement is as follows.

- We start from the FEM equation governing the equilibrium of a single scissors unit in which we separate the external and internal degrees of freedom in order to obtain the matrix equation:

$$
\begin{bmatrix} K_{ee} & K_{ei} \\ K_{ie} & K_{ii} \end{bmatrix} \begin{bmatrix} q_{e} \\ q_{i} \end{bmatrix} = \begin{bmatrix} f_{e} \\ f_{i} \end{bmatrix}, \tag{20}
$$

where the index 'e' denotes external degrees of freedom and 'i' denotes the internal ones. Thus, the partial stiffness matrix, K_{ee} collects reactions in external dofs resulting from displacements at external dofs, K_{ei} collects reactions in external dofs resulting from displacements at internal dofs, K_{ie} collects reactions in internal dofs resulting from displacements at external dofs and, eventually, K_{ii} collects reactions in internal dofs resulting from displacements at internal dofs. Consequently, q_{e} and q_{i} denote generalized displacements at external and internal dofs, respectively, while f_{e} and f_{i} denote concentrated forces and moments at external and internal dofs, respectively.

- Firstly, we separate the subsystem describing equilibrium of the internal node, which can be used to determine generalized displacements q_{i} (two displacements and two rotations

at central pivot) in terms of generalized displacements q_e (two displacements and one rotation at each end of scissors members):

$$q_i = K_{ii}^{-1}\left(f_i - K_{ie}q_e\right). \tag{21}$$

- Secondly, we separate the subsystem describing equilibrium of the external nodes and use the result (21). The resulting equation takes the form:

$$\left(K_{ee} - \widetilde{K_{ei}}K_{ie}\right)q_e = f_e - \widetilde{K_{ei}}f_i, \tag{22}$$

where $\widetilde{K_{ei}} = K_{ei}K_{ii}^{-1}$. Eq. (22) can be written in a shorter form:

$$\widetilde{K_{ee}}\, q_e = \widetilde{f_e}, \tag{23}$$

where $\widetilde{K_{ee}} = K_{ee} - \widetilde{K_{ei}}K_{ie}$, $\widetilde{f_e} = f_e - \widetilde{K_{ei}}f_i$ and it can be considered as equilibrium equation for scissors unit superelement. The matrix K_{ii} is a diagonal matrix, which contains two displacements and two rotations at the central pivot. All diagonal components of this matrix are non-zero (diag $[K_{ii}] \neq 0$) and thus it has the inverse matrix K_{ii}^{-1}. In the case of small value of any diagonal component of matrix K_{ii} it is hard to find the stiffness matrix $\widetilde{K_{ee}}$ and external loading $\widetilde{f_e}$ for the superelement due to numerical errors. Except this case, it is possible to determine deformation of the scissors unit using the superelement method.

Let us note that the size of the stiffness matrix of the superelement is determined by the number of external degrees of freedom. Thus, superelement stiffness matrix $\widetilde{K_{ee}} \in \mathbf{R}^{12\times12}$, while the classical stiffness matrix of the scissors unit $K \in \mathbf{R}^{16\times16}$.

From the mathematical point of view the procedure of deriving the scissors unit superelement allows to reduce the size of the problem and to diminish the dimension of the inverted stiffness matrix. In the case of scissors unit section the procedure of deriving the superelement can be conducted fully analytically and allows to obtain algebraic formulae defining particular components of the stiffness matrix of the superelement. This enables fast generation of the superelement stiffness matrix for various geometrical and material data.

The methodology of assembling the model of the Mobile Bridge (or any other scissors structure) using superelements is analogous to the procedure of assembling it using standard stiffness matrices of single scissors units. The main difference is that smaller matrices are used and hence assembling of the global stiffness matrix is facilitated. The advantage of the superelement method is reduction of the total number of degrees of freedom in analyzed mechanical system and decrease of the corresponding cost of numerical solution. In turn, the disadvantage is the requirement of conducting additional computations including preliminary determination of superelement stiffness matrix and reconstruction of internal degrees of freedom displacements after the main part of FEM solution. At the current stage of research we have decided not to continue the study on superelement approach and to focus on developed FEM methodology. Nevertheless the superelement approach can be incorporated into arbitrary FEM software such as ABAQUS or LsDyna, which creates possibilities of its versatile application.

7. Numerical computations

7.1. Validity of the proposed FEM. The stiffness matrix of all scissor and/or all reinforcement struts in the GCS is shown in Eq. (17) or Eq. (19) based on the connection conditions of each unit. Using the boundary conditions and load conditions from this stiffness matrix, based on Eq. (9), the nodal displacement can be obtained by the stiffness equation:

$$u = K_{sc}^{*\,-1}f. \tag{24}$$

If the scissors element has no reinforcements, it is possible to directly use the equation $u = K_{sc}^{-1}f$. By returning the displacements to the ECS, the sectional forces of each member can be obtained as follows:

$$\overline{p}^m = k^{(m)}\,\mathscr{T}_m^{\mathrm{T}}u^m,$$

$$\begin{bmatrix} \overline{p}_i^m \\ \overline{p}_j^m \end{bmatrix} = \begin{bmatrix} k_{ii}^{(m)} & k_{ij}^{(m)} \\ k_{ji}^{(m)} & k_{jj}^{(m)} \end{bmatrix} \mathscr{T}_m^{\mathrm{T}} \begin{bmatrix} u_i^m \\ u_j^m \end{bmatrix}, \tag{25}$$

where $\overline{p}_\bullet^m$ and $u_\bullet^m$ with $\bullet = i$ or j stands for ends of element of a member m which has the following components:

$$\overline{p}_\bullet^m = \left[fx_\bullet^m,\ fy_\bullet^m,\ M_\bullet^m,\ \overline{M}_\bullet^m\right]^{\mathrm{T}},$$

$$u_\bullet^m = [u_\bullet^m,\ v_\bullet^m,\ \varphi_\bullet^m,\ \overline{\varphi}_\bullet^m]^{\mathrm{T}}.$$

These variables are corresponding to Fig. 3. The $\overline{p}^m$ calculated by Eq. (25) is the vector of the sectional forces, such as the axial force (N_m), shear force (Q_m), and bending moment (M_m) in the ECS. The validity of this method was assessed by comparing it with the values calculated using the theory of equilibrium mechanics, which produces forces consistent with the experimental results [11, 12].

As an example of the benchmark model, we consider the three units of the scissors structure supported at the ends as the boundary condition shown in Fig. 4. This scissors model becomes internally unstable in the truss member that has the double rotations of degrees-of-freedom at the pivot centre point which depends on zero-stiffness problem of geometrical configuration or supports condition, hence it cannot be solved as a numerical model. However, because the rigid frame element, as opposed to the scissors element, can be stably obtained as a numerical model, the models are compared and verified, as in section 7.3. Analysis was conducted on this end-supported analytical model, assuming that it was deployed with an angle
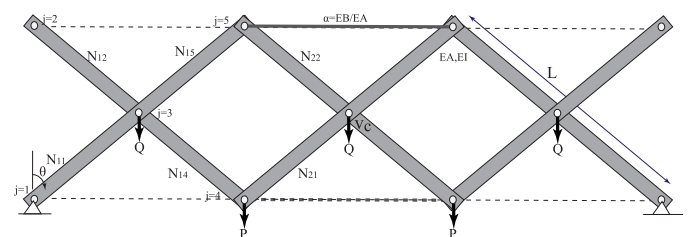
Fig. 4. The three-scissor units with/without several reinforced struts on the both ends hinge support with loads Q and P

I. Ario, T. Yamashita, Y. Chikahiro, M. Nakazawa, K. Fedor, C. Graczykowski, and P. Pawłowski

of $\theta = 45°$. The loads consisted of a live load P and a dead weight Q of a scissors unit. The analytical parameters and material properties used are presented in Table 1. For this numerical model of the scissors structure, it is possible to construct a set of stiffness matrices $K_{sc}^{(M)}$ for a scissors element on the SCI from Eq. (15). The numerical analysis is developed using a FORTRAN program based on this method and the components of the stiffness matrix $K_{sc}^{(1)} = K_{sc}^{(2)} = K_{sc}^{(3)}$. The scissor stiffness components of $\sum_{m=1}^{4} k_{33}^{(m)}$ of Eq. (15) on the SCI unit are as follows:

$$\sum_{m=1}^{4} k_{33}^{(m)}$$
$$= \begin{bmatrix} 0.111E+06 & 0.000E+00 & 0.000E+00 & 0.000E+00 \\ 0.000E+00 & 0.111E+06 & 0.000E+00 & 0.000E+00 \\ 0.000E+00 & 0.000E+00 & 0.263E+09 & 0.000E+00 \\ 0.000E+00 & 0.000E+00 & 0.000E+00 & 0.263E+09 \end{bmatrix}, \quad (26)$$

where the underlined third and forth diagonal components of the scissors's stiffness matrix are the same rotational stiffness values. The CPU time used for the computing of the three-unit model was real: 0 m 0.096 s, using the command time on the Linux system[3].

Table 1
The analytical parameters of the three-scissor units

Length of the scissor member L (mm)	1000
Cross-sectional area of the scissor member A (mm^2)	384
Deployment angle θ ($°$)	45
Elastic modulus of the scissor units E_{al} (GPa)	70
Sectional moment of inertia I(mm^4)	234592
Elastic modulus of the steel reinforcement E_{st} (GPa)	200
Load P (N)	1000
Weight of the scissors unit Q (N)	1000
Stiffness ratio between the scissor units and their reinforcement α	0.1

The set of four degrees of freedom from the left of the matrix component corresponds to the node numbers $j = 1, \cdots, 5$ in the scissors element. It is found that there are four degrees of freedom including two independent rotations for each nodal point because the expanding degree of the left (or right) nodal connections of the scissors element are connected to the neighbouring units for two different rotational displacements. The exceptions are the external nodes at each end, where the extra degrees of freedom are not filled by the component of the stiffness matrix of the neighbouring unit. To solve Eq. (24), the

[3]The computer specifications were AMD Athlon(tm) II Neo N36L Dual-Core Processor, 800 MHz, 16GB RAM, running pgfortran 19.10-0 LLVM 64-bit on x86-64 Linux.

mentioned additional degrees of freedom of the external nodes do not have to be treated as fixed boundary conditions. These independent external rotations will always be zero and do not have to be included in the numerical computations.

There are several reinforcement patterns for this scissors structure which will be described in the next section. Here, to verify the analytical accuracy, the displacement value of the scissor structure reinforced only in the upper centre position, which is calculated using FEM, is compared to the value obtained from equilibrium mechanics and results from the FEM software ABAQUS.

The position of the reinforced strut is at the upper centre, which is drawn as a solid line in Fig. 4. Using these analysis conditions, we obtained the numerical results from two analysis methods: the theory of equilibrium mechanics and FEM presented method (Table 2). Moreover, we compared these results with the ABAQUS calculation (Table 3). Details of the ABAQUS model are presented in Section 8. We only present the results of axial force for each element (although we obtained the internal forces Q_j^k and M_j^k), as the axial force results for members located in the left–right symmetrical positions were the same. The difference between the equilibrium result and that obtained by the FEM analysis and ABAQUS computations was small, thereby confirming the validity of the FEM.

Table 2
The axial force results for the 3 units of scissors structure with the reinforcement in the upper central section

Number of axial force	The present method (N)	Equilibrium mechanics (N)	Difference (N)	Percentage (%)
N_{11}	−2890.353	−2890.350	−0.003	0.00010
N_{15}	−2183.247	−2183.250	0.003	−0.00014
N_{12}	0.000	0.000	0.000	0.00000
N_{14}	583.254	583.254	0.000	0.00000
N_{21}	707.107	707.107	0.000	0.00000
N_{22}	1661.919	1661.919	0.001	0.00006

Table 3
The axial force results for the 3 units of scissors structure with the reinforcement in the upper central section. Used profile is rectangular with 25 mesh elements for each beam

Number of axial force	ABAQUS software (N)	Equilibrium mechanics (N)	Difference (N)	Percentage (%)
N_{11}	−2891.900	−2890.350	−1.550	−0.05349
N_{15}	−2184.790	−2183.250	−1.540	−0.07062
N_{12}	0.000	0.000	0.000	0.00000
N_{14}	580.159	583.254	−3.095	−0.53347
N_{21}	707.107	707.107	0.000	0.00000
N_{22}	1668.110	1661.919	−6.192	0.37114

1326

The stiffness matrix from Eq. (11) is a stiffness matrix for a Bernoulli beam. An analogous procedure as presented in Section 3 was implemented for a Timoshenko beam. The results obtained for the central displacement were 1.897% higher.

7.2. Effects of reinforcement for the scissors structure. The reinforcement was analysed using several conditions. First, the influence of reinforcement on stress distribution was observed using the parameters presented in Table 1 and the loading was conditioned as shown in Fig. 4. This analysis was performed by manipulating the cross-section area ratio between reinforcement and standard members of the scissor structure. The weight of the reinforcement material was ignored, and the maximum bending moment, axial force, compressive stress, and bending stress were obtained. The maximum axial force was determined to occur for the maximum cross-section area ratio between reinforcement and the scissor structure, and the maximum bending moment occurred for a minimum cross-section area ratio between them. Using a parameter ratio of α, the stiffness of the reinforced strut is $EB = \alpha EA$. Here, EA is the stiffness for the main scissors frame. Therefore, a trade-off between these two values was determined. Before adding the reinforcing member, the maximum bending stress was higher than the maximum axial stress, indicating that the bending stress should be reduced. The bending stress obtained after reinforcement was lower than that obtained before reinforcement.

Second, when effective displacement suppression is considered for the same boundary conditions as in Table 1 and loading conditions as in Fig. 4, the suppression effect of vertical displacement is evaluated for different types of reinforcement material. Two types of reinforcement materials were used in this analysis: aluminium alloy (as $E = E_{al}$) and steel (as $E = E_{st}$). In this analysis, we assumed that the weight of reinforcement material was ignored. The results of the analysis are shown in Fig. 5. As seen in Fig. 5(a), the central displacement was reduced to 90% after reinforcement was made of aluminium alloy. Likewise, Fig. 5(b), in which using $\alpha = 0.1$, shows the central displacement reduction after reinforcement was made of steel. This reduction was 48.5% greater than in the situation of using aluminium alloy, thereby indicating that steel is a superior reinforcement material in comparison to aluminium alloy.

Next, this analysis explains the influence of the location of reinforcement. The system parameters are defined in Table 1, loading condition is depicted in Fig. 4 and the aluminium alloy is used as the reinforcement. The analysis was conducted using 5 cases: no reinforcement, only one reinforcement member in the upper center position, only one reinforcement member in the bottom center position, all possible reinforcement members in the upper span, and all possible reinforcement members in the bottom span. In this analysis, the own weight of the possible reinforcement members is ignored. The result is presented in Table 4. From the result, we can conclude that central displacement is higher in cases of reinforcement in the case of bottom and no reinforcement than in the case of the reinforcement in the upper span. There are 2 types of upper span reinforcement possible and their differences are shown in Table 4. Therefore, upper span is a better suited location of reinforcement. This re-

Disp. v_c (mm) at the central pivot
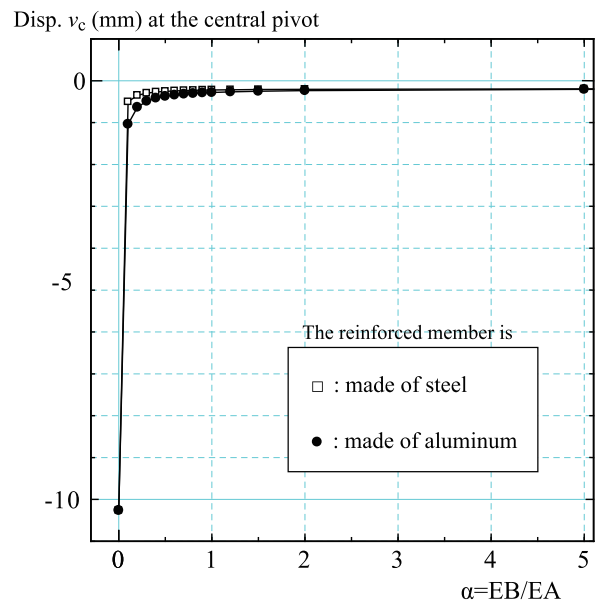
(a) The effect of the reinforcement

Disp. v_c (mm) at the central pivot
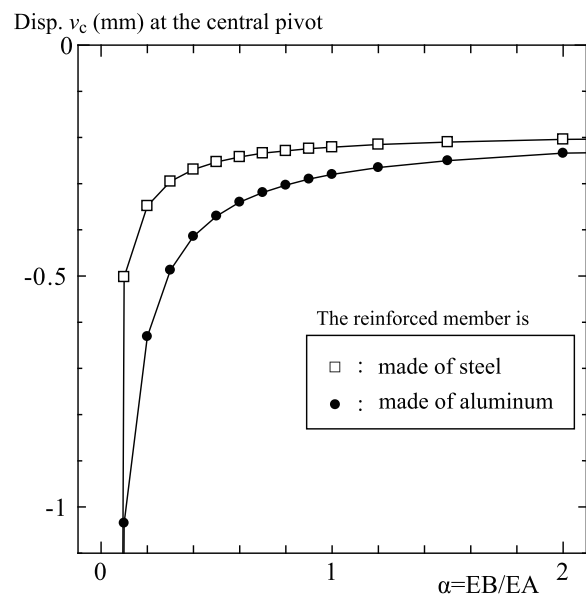
(b) Zooming up the range

Fig. 5. The central vertical displacements obtained using steel and aluminium alloy reinforcement materials with a cross-sectional area ratio between reinforcement and scissors structure α

sult is analogous to the result in previous analysis, however, this analysis considers the own weight of the structure. The analysis indicates that considering the own weight increases the central displacement, maximum moment, and maximum axial force. In the case of reinforcement of the entire upper span, the central displacement of the scissor structure is larger than in the case of single reinforcing member located in the centre.

We obtain the results of the internal sectional forces by this method as shown in Fig. 6. The model is equipped with only one reinforcement member with characteristic parameter $\alpha = 0.1$ at the upper central position. Fig. 6(a) is the Ax-

I. Ario, T. Yamashita, Y. Chikahiro, M. Nakazawa, K. Fedor, C. Graczykowski, and P. Pawłowski

Table 4
The results depending on location of reinforcement (as $\alpha = 0.1$)

Location of reinforcements	No reinforcement		at the upper centre		at the bottom centre		all in the upper		all in the bottom	
Type of calculation	Present SCI. FEM	ABAQUS	Present SCI. FEM	ABAQUS	Present SCI. FEM	ABAQUS	Present SCI. FEM	ABAQUS	Present SCI. FEM	ABAQUS
Central disp. (mm)	10.261	10.483	1.036	1.037	10.261	10.483	0.938	0.940	10.261	10.483
Max. bending moment (Nmm)	7.07×10^5	7.07×10^5	3.23×10^5	3.22×10^5	7.07×10^5	7.07×10^5	2.60×10^5	2.54×10^5	7.07×10^5	7.07×10^5
Max. axial force (N)	-2.12×10^3	-2.12×10^3	-3.26×10^3	-3.27×10^3	-2.13×10^3	-2.12×10^3	-3.02×10^3	-3.02×10^3	-2.12×10^3	-2.12×10^3
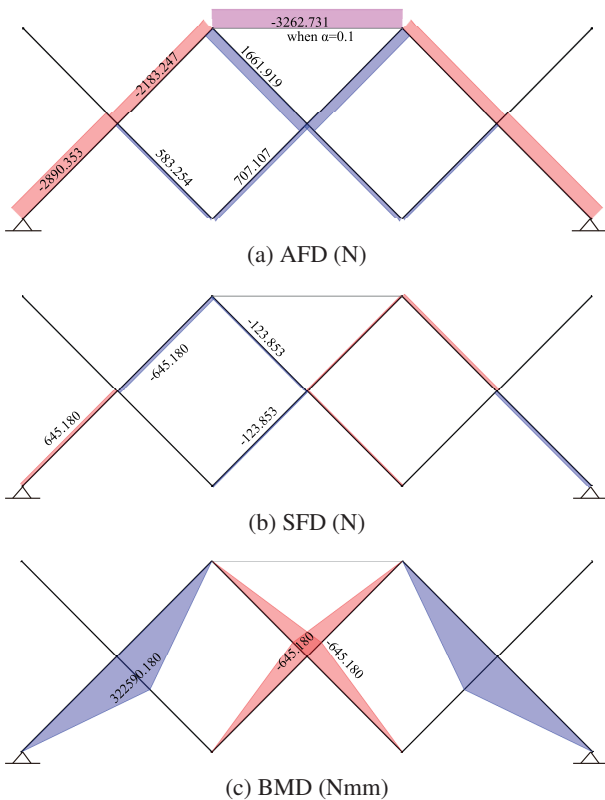
Fig. 6. The results of internal sectional forces with the reinforcing strut
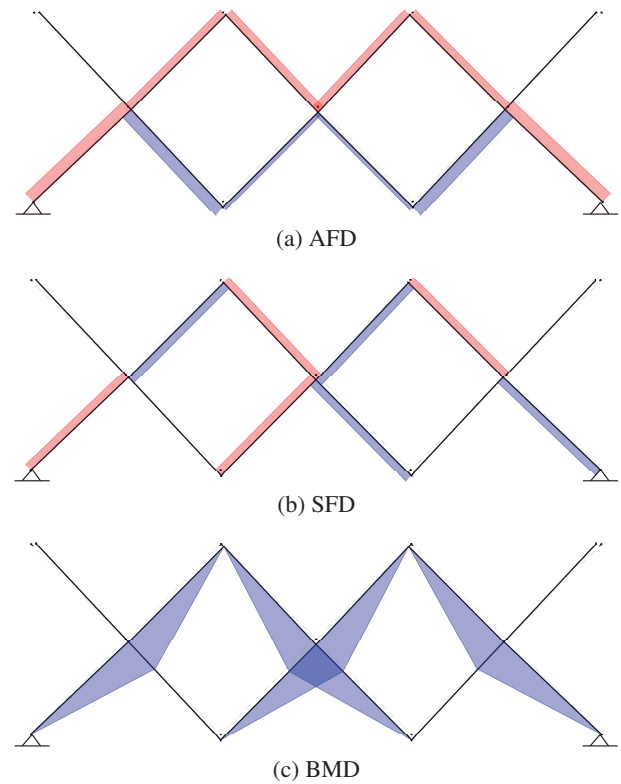
Fig. 7. Three-scissors units without a reinforcing strut

ial Force Diagram, Fig. 6(b) is the Shear Force Diagram and Fig. 6(c) is the Bending Moment Diagram. The member of this bridge is rather a frame element which has a part of force distributions such as Axial Force Diagram (AFD), Shearing Force Diagram (SFD), and Bending Moment Diagram (BMD).

The magnitude of the intersectional forces in the scissors model without any reinforcement is shown in Fig. 7. It is found that there are upper compression members and lower tension members in the AFD, as shown in Fig. 7(a). In Fig. 7(c), large positive values of BMD are seen for each unit without reinforcement.

7.3. Comparison with Rigid Frame Models. To compare not only the scissors model but also the versatility of the proposed analytical method, an examplary of analysis of a rigid frame model is presented. In this case, the two independent rotational

displacements of the scissors connection correspond to the degrees of freedom of the common rotational displacement; the analytical conditions, such as boundary conditions and load conditions, are almost the same as those of the scissors model.

For the numerical model of the scissors structure, it is possible to build a set of stiffness matrices $K_{sc}^{(M)}$ for a frame element of the SCI from Eq. (15). In the numerical analysis of this rigid frame structure, the size of the stiffness matrix is reduced so that $K_{sc}^{(1)} = K_{sc}^{(2)} = K_{sc}^{(3)}$. The rigid stiffness components of $\sum_{m=1}^{4} k_{33}^{(m)}$ of Eq. (15) on the SCI unit is as follows:

$$\sum_{m=1}^{4} k_{33}^{(m)} = \begin{bmatrix} 0.111E+06 & 0.000E+00 & 0.000E+00 \\ 0.000E+00 & 0.111E+06 & 0.000E+00 \\ 0.000E+00 & 0.000E+00 & \underline{0.525E+09} \end{bmatrix}.$$

The set of the three degrees of freedom from the left of the matrix component corresponds to the node numbers $j = 1, \cdots, 5$ in the frame (scissors) element. It is found that there are three degrees of freedom including the common rotations for each nodal point because the element does not expand as in the ordinary finite element. The first and the second diagonal components of the stiffness matrix for the rigid frame and for the scissors are corresponding to $0.111E + 06$. The third component of the stiffness matrix for the rigid frame is corresponding to the sum of two rotational stiffness for the scissors Eq. (26) as follows:

$$\underline{0.525E + 09} = \underline{0.263E + 09} \times 2.$$

Fig. 8 shows the analytical results of the rigid frame model without reinforcement. Fig. 8(a) shows the axial force, Fig. 8(b) shows the shear force, and Fig. 8(c) shows the bending moment diagram, respectively. Comparing the analysis results of scissors in Fig. 7, the distribution of axial force in Fig. 8(a) was almost the same axial force distribution in the form of 'M' for the compression distribution and in the form of 'W' for the tension distribution. The shear force in Fig. 8(b) is also similar to the SFD of scissors. BMD in Fig. 8(c), unlike the result of the moment value is 0 at the connection end of the scissors member of Fig. 8(c), the moment is the largest in the centre of the section.

The frame structure of three units

(a) AFD

(b) SFD

(c) BMD
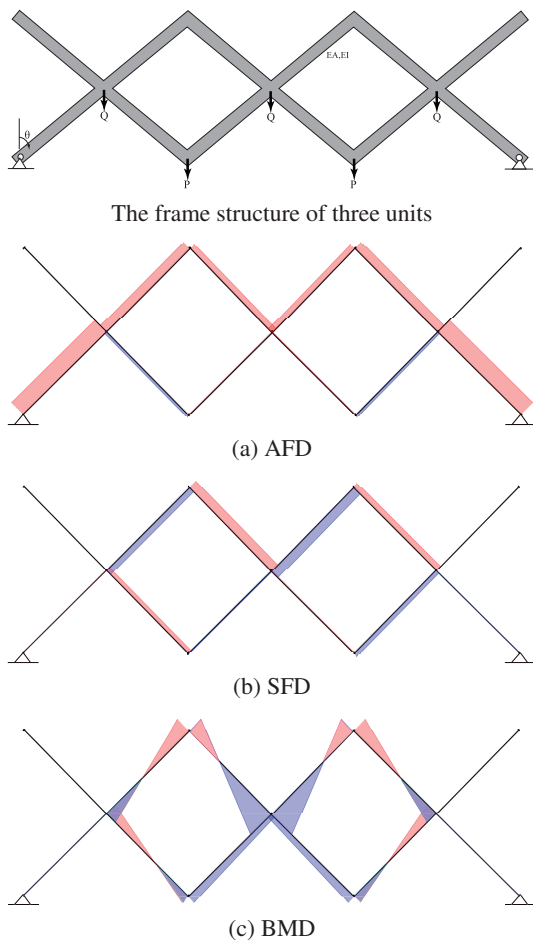
Fig. 8. Rigid frame results without the reinforcing strut on both end supports

The moment at the centre of the model is positive and matches its left and right ends values and is partly similar to the BMD of scissors. Fig. 9 shows the cross-sectional force diagrams of the upper chord member ($\alpha = 0.1$) stiffened only in the central spacing resisting only the axial force. The AFD in Fig. 8(a) had almost the same distribution form as that in the case of stiffened scissors in Fig. 6. BMD in Fig.6(c) becomes smaller than the distribution value of scissors, and it can be seen that positive and negative values are arranged in a well-balanced manner.

The frame structure of three units with a reinforcement

(a) AFD

(b) SFD

(c) BMD
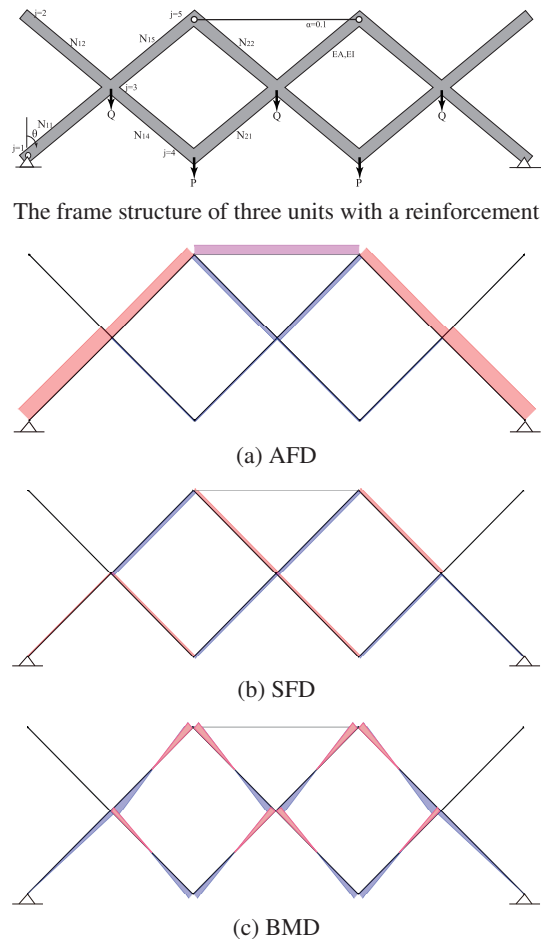
Fig. 9. Rigid frame results with the reinforcing strut supported on both ends

8. Modelling by ABAQUS

ABAQUS 6.13-1 was used for the calculations. Because of the nature of the analysed benchmark model, 2D beam element B21 in a 2-node linear beam was used in the computations. The parts used in the models were 2D beam elements with an Multiple Point Connection (MPC) between the beams. In the MPC pin type connection, the displacement degrees are fixed while the rotational degrees are free. Two beams of a single scissors section are not located at the same vertical plane so they pass each other in space. The material and geometrical characteristics of the model are compatible with the information presented in Table 1.

In general we obtained very good agreement of results of presented methodology with results from Abaqus modelling. We observed that for different types of profiles with the same cross-sectional area A and sectional moment of inertia I, the results are slightly different and we presented them as a comparison of the central displacement in Fig. 10. The stiffness matrix used in the FEM method in Eq. (11) is in fact the stiffness matrix for the Bernoulli beam, nevertheless we included also comparison with Timoshenko beam. In the software calculations, we obtained results for three different profiles: generalized, rectangular and box. In every case, the results were convergent for 25 mesh elements for each beam in the model.

(a) Numerical and ABAQUS modeling

(b) Percentage difference to numerical calculation of the Bernoulli beam
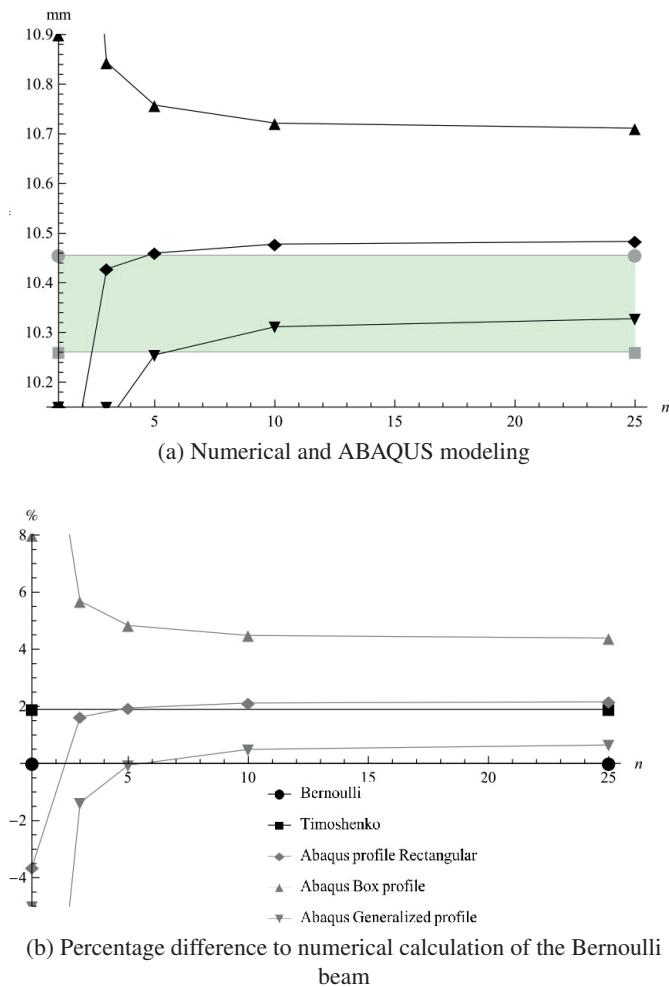
Fig. 10. Central vertical displacements obtained using numerical computation wtih Bernoulli and Timoshenko beam element and ABAQUS software with different type of profiles and different numbers of mesh elements n

The minimum difference of central displacement was between the presented method applied for the Timoshenko beam and the ABAQUS software calculation with a rectangular profile and it was 0.26%. The most closely aligned results to the presented method applied for the Bernoulli beam was the ABAQUS software calculation with a generalized profile, with a difference of 0.65%.

The ABAQUS computation includes more degrees of freedom in the stiffness matrices, and therefore, calculations are more complicated and computationally demanding than our model. The computation of the presented benchmark model using the FEM method in Mathematica 9.0.1. software took 1.04 s, while in the ABAQUS software, it took 26.12 s.

8.1. Influence of friction. To evaluate the influence of friction in the connection nodes between the beams, we changed the type of pin connections from an MPC pin to a basic joint rotation with a friction coefficient. In general, the friction coefficient depends on the combination of materials and surface conditions. The static friction coefficient for friction between aluminium alloy and aluminium alloy on clean and dry surfaces varies in the range 1.05–1.35. Similarly friction coefficient for aluminum on steel in dry condition of Mobile bridge is approximately less 0.65. The influence of the variation between 0 and 1.4 is minimal, as presented in Fig. 11(a).

(a) Realistic range of the friction coefficient

(b) Influence of large friction coefficient modeling mechanical blockage of rotations in joints
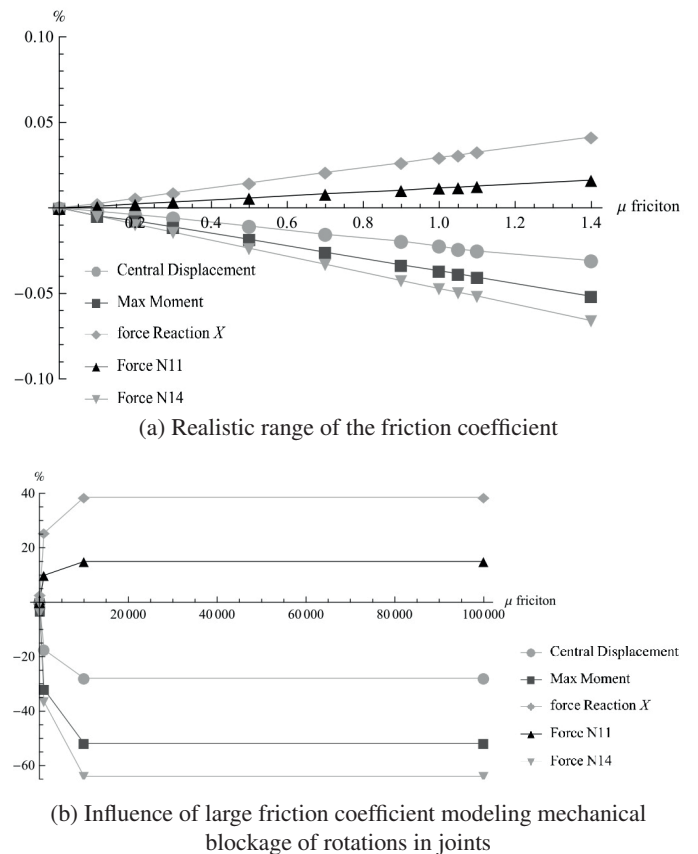
Fig. 11. Influence of the friction coefficient on static response of Mobile Bridge

Potential mechanical blockage of rotation in all connections between the beams is modelled as an extreme friction coefficient and presented in Fig. 11(b). In such a hypothetical situation, the central displacement was reduced by 28%, while a significant increase was noticed only in the x-direction reaction force.

Table 5
The comparison of basic features of the proposed modelling methods

Type of the calculation	Equilibrium mechanics model	Developed models of scissors structures by present method as SCI. FEM	ABAQUS FEM models
Type of structure analyzed	Statically determinate (Stress method)	Statically (in-)determinate (Displ. method)	Statically (in-)determinate (Displ. method)
Type of structural analysis	Static (buckling)	Static Possibly: natural frequency, buckling transient dynamics	Static, buckling, natural frequency, transient dynamics, fully nonlinear
Number of finite elements required	N/A	2 elements for each beam 4 elements for each unit 12 elements for 3-unit MB	10–20 elem. for each beam 20–40 elem. for each unit 120–240 elem. for 3-unit MB
Effort of model preparation	Small: assembling of the equilibrium equations	Small due to usage of scissors units stiffness matrices and assembly parameterization	Larger due to requirement of introducing the entire geometry from scratch and application of special techniques of joint modelling
Cost of numerical analysis	Very small: solution of small system of algebraic equations to determine forces & application of Maxwell-Mohr formula to determine displ.	Still very small: solution of slightly larger system of algebraic equations to determine displ./rotat. & matrix multiplication to determine internal forces	Significantly larger due to increased number of finite elements/degrees of freedom and occurrence of nonlinear phenomena (joints friction, large deformations)
Results possible to be obtained	Internal forces (AFD, SFD, BMD), reactions, strains, displacements	Displacements, strains, internal forces (AFD, SFD, BMD), reactions	Displacements, strains, internal forces (AFD, SFD, BMD), reactions, contact forces, friction force and backlash effects in joints
Model application	Theoretical /educational (only statically determinate structures)	Preliminary engineering analysis, fast design evaluation, optimization, control development	Final engineering analysis, detailed analysis of sophisticated nonlinear response, detailed analysis of local effects in joints

Although the proposed FEM model of the Mobile Bridge[4] takes into account dry friction in joints, it still can be considered as strongly simplified since it neglects the complexity of joints operation resulting from the occurrence of geometrical imperfections, various contact conditions, clearance and backlash. Thus, the proposed FEM models are planned to be further expanded by implementing more complex models of joints, which will precisely capture possible nonlinear phenomena that may occur during joint's surfaces interaction. Both the micromechanical models precisely simulating the effects arising at a single joint and their macromechanical counterparts which can be applied in global models of scissors structures are planned to be developed. Mentioned nonlinear phenomena are expected to be especially important for the numerical analysis of large deformation of Mobile Bridge subjected to critical loads and analysis of its transient dynamic response resulting from exploitative or environmental loads. We assume that a friction parameter of Mobile bridge with the lubricating oil inside at the pin-connection is very small.

---

[4]Since the pin joint-connection part of the Mobile bridge stores the lubricating oil inside, the friction of the pin contact surface is as small as possible, the actual resistance is small, and the influence of the inclination is more sensitive than that.

9. Conclusion

By using the periodicity of scissor structures to construct a standard element for the single scissor unit, we developed a new hierarchical FEM to analyse these systems. The accuracy of the proposed method was demonstrated by analysing the axial force of each member and comparing it with the results obtained by using the theory of equilibrium mechanics and ABAQUS software computation.

Suitable reinforcement pattern depends on the material of the reinforcing member, its cross-sectional area and its position. The difference in the central displacements for different scissors conditions was also investigated. It was determined that steel reinforcing member placed at the centre of the upper span was superior to aluminium one and resulted in the best reinforcement of the scissors structure. It was also found that there is a difference in the internal forces distribution in comparison with the forces in a rigid frame elements without any pin connections. The significant result of our study is the analysis of scissors structures, including frame elements with pin-frame connections for the periodic modular elements, using the FEM.

Finally, this paper summarizes the main merits and compares three present analysis methods including equilibrium mechanics model, developed models of scissors structures and ABAQUS FEM models in Table 5.

I. Ario, T. Yamashita, Y. Chikahiro, M. Nakazawa, K. Fedor, C. Graczykowski, and P. Pawłowski

References

[1] F.Y. Yeh *et al*., "A novel composite emergency bridge for disaster rescue", *The 15th World Conference on Earthquake Engineering* (15WCEE), Lisbon, Portugal (2012).

[2] A.M.A.J. Teixeira, M.S. Pfeil, and R.C. Battista, "Structural evaluation of a GFRP truss girder for a deployable bridge", *Compos. Struct*. 110, 29–38 (2014).

[3] W. Krason and J. Malachowski, "Field test and numerical studies of the scissors-AVLB type bridge", *Bull. Pol. Ac.: Tech*. 62(1), 103–112 (2014).

[4] H.H. Hung, Y.C. Sung, K.C. Chang, S.H. Yin, and F.Y. Yeh, "Experimental testing and numerical simulation of a temporary rescue bridge using GFRP composite materials", *Constr. Build. Mater*. 114, 181–193 (2016).

[5] O. Benjeddou, O. Limam, and M. B. Ouezdou, "The experimental and the theoretical analysis of the serviceability behavior of a deployable footbridge", *Arch. Civ. Mech. Eng*. 17(2), 293–306 (2017).

[6] T. Lewiński, T. Sokół, and C. Graczykowski, *Michell Structures*, Springer, 2019.

[7] Y. Wang, A.P. Thrall, and T.P. Zoli, "Adjustable module for variable depth steel arch bridges", *J. Constr. Steel. Res*. 126, 163–173 (2016).

[8] A. Beukers and Ed. Van Hinte, *The Inevitable Renaissance of Minimum Energy Structures*, 010 publishers, Rotterdam 2005.

[9] C. Graczykowski and P. Pawlowski, "Mathematical Modelling of Adaptive Skeletal Structures for Impact Absorption and Vibration Damping", *Procedia Eng*. 199, 1671–1676 (2017).

[10] I. Ario, M. Nakazawa, Y. Tanaka, I. Tanikura, and S. Ono, "Development of a prototype deployable bridge based on origami skill", *Autom. Constr*. 32, 104–111 (2013).

[11] Y. Chikahiro *et al*., "Experimental and numerical study of fullscale scissor type bridge", *Autom. Constr*. 71(2), 171–180 (2016).

[12] Y. Chikahiro, I. Ario, and M. Nakazawa, "Theory and Design Study of a Full-Scale Scissors-Type bridge", *J. Bridge Eng. (ASCE)* 21(9), (2016).

[13] N. Veuve, A.C. Sychterz, and I.F.C. Smith, "Adaptive control of a deployable tensegrity structure", *Eng. Struct*. 152, 14–23 (2017).

[14] Y. Chikahiro *et al*., "Dynamics of the scissors-type Mobile Bridge", *Procedia Eng*. 199, 2919–2924 (2017).

[15] Y. Chikahiro, I. Ario, P. Pawłowski, C. Graczykowski, and J. Holnicki-Szulc "Optimization of reinforcement layout of scissor type bridge using differential evolution algorithm", *Comput.-Aided Civil Infrastruct. Eng*. 34(6), 523–538 (2019).

[16] M.J. Turner, R.W. Clough, H.C. Martin, and L.J. Topp, "Stiffness and Deflection Analysis of Complex Structures", *Int. J. Aeronaut. Sci*. 23(9), 805–823 (1956).

[17] K. Ikeda and K. Murota, *Imperfect Bifurcation in Structures and Materials: Engineering Use of Group-Theoretic Bifurcation Theory*, Springer-Verlag, New York, 2002.

[18] F. Kovács, "Extended truss theory with simplex constraints", *Int. J. Solids Struct*. 48(3–4), 472–482 (2011).

[19] C.T. Sun and R.S. Vaidya, "Prediction of composite properties from a representative volume element", *Compos. Sci. Technol*. 56(2), 171–179 (1997).

[20] I. Ario and M. Nakazawa, "Analysis of multiple bifurcation behavior for periodic structures", *Proc. of 4th Polish Congress of Mechanics and 23rd International Conference on Computer Methods in Mechanic*, Krakow, Poland (2019).

[21] I. Ario and M. Nakazawa, "Analysis of Multiple Bifurcation Behaviour for Periodic Structures", *Arch. Mech*. 72(4), 1–24 (2020).

[22] D. Hower, S. Yu, T.M. Ricks, B.A. Bednarcyk, and J. Simon, "Weave geometry generation avoiding interferences for mesoscale RVEs", *J. Mater. Sci. Technol*. 35(12), 2869–2882 (2019).

[23] I. Ario, Y. Chikahiro, M. Nakazawa, J. Holnicki-Szulc, P. Pawlowski, and C. Graczykowski, "Structural Analysis of a two-unit of Scissors Structure", *Proc. of Solid Mechanics (Solmech)*, Warsaw, Poland (2016).